DØ Note 5893-CONF

Measurement of the W Boson Mass with 1 fb^{-1} of DØ Run II Data

The DØ Collaboration
URL http://www-d0.fnal.gov
(Dated: May 4, 2009)

We present a measurement of the W boson mass using DØ data collected from 2002 to 2006 corresponding to 1 fb^{-1} of data. This yields 499,830 $W \to e\nu$ candidates. We measure the mass using the transverse mass, electron transverse momentum and missing transverse energy distributions. These three results are combined to give

$$m_W = 80.401 \pm 0.021 \text{ (stat)} \pm 0.038 \text{ (syst) GeV} = 80.401 \pm 0.043 \text{ GeV}.$$

Preliminary Results for Winter 2009 Conferences

I. INTRODUCTION

Knowledge of the W boson mass is currently the limiting factor in our ability to tighten the constraints on new physics that couples to the electroweak (EW) sector. Improving the measurement of m_W, then, is an important contribution to our understanding of the electroweak interaction, and, potentially, of how electroweak symmetry is broken. The current world-average measured value of the W mass is $m_W = 80.399 \pm 0.025$ GeV [1][22]. This result is a compilation of measurements from the four LEP experiments, ALEPH [2], DELPHI [3], L3 [4], and OPAL [5], and results from DØ [6] and CDF [7] at the Tevatron, including a Run II result from CDF [8], $m_W = 80.413 \pm 0.034(\text{stat.}) \pm 0.034(\text{syst.})$ GeV.

This note presents a measurement of the W boson mass using data taken from 2002-2006 with the DØ detector [9], corresponding to a total integrated luminosity of 1 fb^{-1}. This measurement is performed using the $W \to e\nu$ decay mode. This channel is chosen because the DØ calorimeter is well-suited for a precise measurement of electron energies, providing an energy resolution of 3.6% for electrons of energy 50 GeV. In $p\overline{p}$ collisions, the longitudinal momentum of the parton-parton center of mass is undetermined. Since the longitudinal momentum of the neutrino from the W decay is also unmeasurable, we use kinematic variables determined in the plane perpendicular to the proton beam direction, rather than a determination of the invariant mass of the W decay products. Three such variables are used in this measurement: the transverse mass, m_T, the electron transverse momentum, p_T^e, and the neutrino transverse momentum p_T^ν. The transverse mass is calculated with the formula

$$m_T = \sqrt{2p_T^e p_T^\nu (1 - \cos(\phi_e - \phi_\nu))}, \tag{1}$$

where ϕ_e and ϕ_ν are the azimuthal angles of the electron and neutrino momentum respectively. The p_T^ν magnitude and direction are inferred from the event missing transverse energy ($\vec{\not\!\!E}_T$). Throughout this analysis, $\not\!\!E_T$ is used to denote both the experimentally measured quantity and the neutrino momentum, and "transverse" means a plane or direction perpendicular to the nominal Tevatron beam direction at DØ.

The m_T and p_T^e measurements are complementary because the major cause of changes from the true to the measured spectrum for each quantity arises from different sources. For the m_T method, the major cause of the change is measurement resolution, while for the p_T^e method, the major cause is the intrinsic W transverse momentum. Thus the two measurements have sensitivity to different components of the analysis. The $\not\!\!E_T$ measurement is sensitive to the same effects as both m_T and p_T^e, but it is not 100% correlated with either, so it still provides additional information.

Because of complex detector acceptance and resolution effects, the shapes of the three measured variables cannot be calculated analytically. Therefore the measurement of m_W is obtained by a comparison of the spectra of the three different measurement variables with templates of the same variable distributions constructed from Monte Carlo simulation with varying input W masses. This requires templates with very high statistics ($\sim 10^8$ events) to characterize the different systematic effects with sufficient precision.

To generate appropriate templates, a fast parametrized Monte Carlo simulation (PMCS) has been developed to produce large samples on a reasonable time scale and to provide a detailed description of the detector performance. $Z \to ee$ events, and sometimes $W \to e\nu$ events, are used to determine the parametrizations, since electrons from Z and W decays are well measured by the calorimeter. This allows a determination of all of the relevant physics parameters, including characteristics of the hadronic recoil system, from the data itself. Since the Z mass and width are known with a high precision from the LEP measurements [10], their values can be used to calibrate the electromagentic calorimeter. Care must be taken to ensure that the calibrations at the Z pole are valid at the somewhat lower average energy of the electrons from W decay. Once this has been established, the W mass measurement is effectively a measurement of the ratio of W and Z masses.

The W mass measurement requires the following components: event generation, including next-to-leading-order photon and gluon radiation; event selection; fast Monte Carlo parametrization including electron efficiency simulation, electron response simulation and recoil response simulation; measurement of the backgrounds; and a comparison between data and templates to determine the W mass. In the following sections, we describe each component along with its systematic uncertainty and then present the mass measurement results.

II. DØ DETECTOR

The D0 detector [9] contains tracking, calorimeter and muon subdetector systems. Silicon microstrip tracking detectors (SMT) near the interaction point cover pseudorapidity $|\eta| \equiv -\ln(\tan(\theta/2)) < 3$ to provide tracking and vertexing information. The central fiber tracker (CFT) surrounds the SMT, providing coverage to about $|\eta| = 2$. A 2 T solenoid surrounds these tracking detectors.

Three uranium-liquid argon calorimeters measure particle energies. The central calorimeter (CC) covers $|\eta| < 1$, and two end calorimeters (EC) extend coverage to about $|\eta| = 4$. The CC is segmented in depth into eight layers. The first four layers are used primarily to measure the energy of photons and electrons and are collectively called the electromagnetic (EM) calorimeter. The remaining four layers, along with the first four, are used to measure the energy of hadrons. Most layers are segmented into 0.1×0.1 regions in (η, ϕ) space. The third layer of the EM calorimeter is segmented into 0.05×0.05 regions.

Muons are measured with stations which use scintillation counters and several layers of tracking chambers over the range $|\eta| < 2$. One such station is located just outside the calorimeters, with two more outside the 1.8 T iron toroidal magnets. Scintillators surrounding the exiting beams mounted on the face of both end calorimeters allow determination of the luminosity. A three level trigger system selects events for data recording at about 100 Hz.

III. EVENT GENERATION

The initial step in constructing templates for extracting the W mass is simulation of W production and decay kinematics using the RESBOS [11] program. RESBOS computes the triple differential cross section $d^3\sigma/dp_T\,dy\,dm$ for Z/γ^* and W processes at hadron colliders. Here p_T is the boson momentum in the plane transverse to the beam, $y = \frac{1}{2}\ln[(E + p_z)/(E - p_z)]$ is the boson rapidity and m is the boson mass. RESBOS uses a gluon resummation calculation for low boson transverse momentum p_T and perturbative QCD calculations at high boson p_T. The W boson p_T spectrum has a significant impact on the simulated p_T^e and p_T^ν spectra so an accurate description of this is an important ingredient of the W mass measurement.

For low p_T W and Z bosons, the main higher order correction to the overall cross section comes from multiple soft and collinear gluon emission which is calculated using the gluon resummation technique. In impact-parameter space resummations, the W p_T spectrum is parametrized using a non-perturbative form-factor using three parameters called g_1, g_2 and g_3. The values of these three parameters need to be determined from experimental data. The Z boson p_T distribution at the Fermilab Tevatron is by far the most sensitive to the value of g_2, has limited sensitivity to g_1, and is quite insensitive to the value of g_3. We use the global fit values listed at Ref. [12] with $g_2 = 0.68 \pm 0.02$ GeV^2 and propagate the uncertainty on g_2 to the W mass measurement. The uncertainties from g_1 and g_3 are negligible.

The dominant effect from EW corrections to the W mass measurement is from radiation of a single photon from the final state charged lepton. The next-largest effect is due to two final state photon radiations. These processes are simulated by combining the PHOTOS program [13] with RESBOS. The PHOTOS program is a universal MC program for final state radition that can generate a maximum of two photons. Systematic uncertainty from radiation has been assessed by comparing the results from PHOTOS with those from WGRAD [14] and ZGRAD [15] which include initial state radiation (ISR) and interference effects but at the one photon level. The overall systematic uncertainty includes: the uncertainty on initial state radiation, final state radiation (FSR), interference between ISR and FSR, and electroweak box diagrams; uncertainty due to the minimum p_T of the FSR photon; and the detector modelling of these radiated photons. The uncertainties are estimated by fitting the sample of events generated without a certain effect to the templates generated with that effect. The final systematic uncertainty on m_W due to all EW corrections is found to be 7 MeV for the m_T method, 7 MeV for the p_T^e method and 9 MeV for the $\not\!\!E_T$ method.

Parton distribution functions (PDFs) enter into the W mass measurement through their effects on the detector acceptance calculation and kinematics of the decay electron. We determine the systematic uncertainty arising from the PDFs using a standard prescription for the CTEQ6.1M [16] parton distribution function. There are 20 free parameters in the CTEQ6M.1 PDF set. For the uncertainty calculation, 40 additional PDFs were defined by CTEQ using positive and negative variation of each parameter until the global χ^2 reached the 90% C.L. We used PYTHIA [17] with PMCS to propagate the variations in the 40 sets to the W mass. We use the formula suggested by the CTEQ authors to determine the uncertainty arising from the PDF sets, but we divide the result from their formula by a factor of 1.6 to convert from a 90% confidence interval to the more standard 68% confidence interval [8]. We did the same analysis using p_T^e and $\not\!\!E_T$ methods. The final uncertainty is found to be 9 MeV for the m_T method, 11 MeV for the p_T^e method and 14 MeV for the $\not\!\!E_T$ method. The uncertainty on the W width contributes a negligible uncertainty to the W mass measurement.

IV. EVENT SELECTION

The data used for this analysis were recorded in the period 2002-2006 and correspond to a total integrated luminosity of 1 fb^{-1}. The average instantaneous luminosity during this period was 41×10^{30} cm^{-2}s^{-1} giving an average of 1.2 interactions per bunch crossing. The data sample is initially defined by requiring candidate events to be recorded via a single-electron trigger. The transverse energy thresholds of the trigger electron varied from 20 GeV to 25 GeV

depending on run conditions, and the shower in the calorimeter arising from the electron candidate was required to have a longitudinal shape consistent with that from an electron. The W or Z production point along the beam line is determined either from the standard primary vertex algorithm or is taken as the projection of the electron track to the beam line if the track is sufficiently far from the point identified by the primary vertex algorithm. Having chosing which definition to use, the production point must satisfy $|z_V| < 60$ cm where z_V is the production position along the beam line with $z_V = 0$ corresponding to the center of the detector.

The decay $W \to e\nu$ is characterized by the presence of a single high transverse momentum electron, missing energy in the plane transverse to the beam which is attributed to the neutrino, and limited additional hadronic energy coming from recoil giving the W boson momentum in the plane transverse to the beam. In addition to the $W \to e\nu$ sample, this analysis requires use of a control sample from the $p\overline{p} \to Z \to ee$ reaction. Candidate $Z \to ee$ events are selected using the same trigger, vertex and electron identification requirements as the W events.

The kinematic requirements for the W selection are:

- one electron reconstructed in the well-instrumented region of the central calorimeter(CC), $|\eta_{det}| < 1.05$ in which η_{det} is the pseudorapidity measured with respect to the center of the detector, passing electron shower shape and energy isolation requirements,
- one track matching the electron with a match probability $P > 0.01$, having at least one silicon microstrip tracker hit and $p_T > 10$ GeV. The match probability is based on the difference in the η and ϕ values of the calorimeter cluster forming the electron and those of the track position at the calorimeter.
- electron $p_T > 25$ GeV,
- $\not\!\!E_T > 25$ GeV,
- $u_T < 15$ GeV and
- $50 < m_T < 200$ GeV

in which u_T is the magnitude of the vector sum of the transverse component of the energies measured in calorimeter cells excluding those associated with the reconstructed electron.

The kinematic requirements for the Z selection are

- two electrons satisfying the calorimeter and track match requirements above. One electron must be reconstructed in the CC, and the other in either the CC or end ($1.5 < |\eta_{det}| < 2.5$) calorimeters,
- both electrons have $p_T > 25$ GeV,
- $u_T < 15$ GeV and
- 70 GeV $\leq m_{ee} \leq 110$ GeV

in which m_{ee} is the invariant mass of the electron-positron pair.

These selections yield 499,830 candidate $W \to e\nu$ events and 18,725 candidate $Z \to ee$ events in which both electrons are in the central calorimeter. The W sample has a signal purity of 96%, but residual backgrounds in the W events are significant and are discussed in Section VI.

V. PARAMETRIZED MONTE CARLO SIMULATION (PMCS)

The W mass is determined by comparisons between data and simulated m_T, p_T^e and $\not\!\!E_T$ distributions. The distributions, made using simulated events, require samples of several 10^8 events, so the DØ standard full GEANT [18] simulation cannot be used. Instead PMCS was developed for this analysis. The electron trigger efficiency, reconstruction efficiency and energy response and resolution are simulated using parametric functions and binned look-up tables. The response and resolution of the hadronic recoil balancing the W boson transverse momentum is also simulated, again using a parametric model. These components of PMCS are described in the following three sub-sections.

The initial input to the simulation uses parametrizations derived from detailed GEANT-based simulation of the DØ detector response to samples of single electrons, $Z \to ee$ events and $W \to e\nu$ events. This GEANT simulation does not describe the detector response with sufficient precision for the W mass measurement, so PMCS is fine-tuned using control data samples. The primary control sample is $Z \to ee$ events. W events are also used in a limited manner for the tuning. In addition to the mean and width of the Z mass distribution, several other variables are used in the tuning. Among the additional variables are those first defined by UA2 [19] and shown in Fig. 1. The $\hat{\eta}$ unit

vector (not to be confused with the pseudorapidity) is coincident with the bisector of the two electron directions in the transverse plane in $Z \to ee$ events (and $\hat{\xi}$ is perpendicular to $\hat{\eta}$). The $\vec{u}_T$ variable represents the hadronic recoil in W production, and the component $u_\parallel$ is the projection onto the electron direction in the transverse plane.

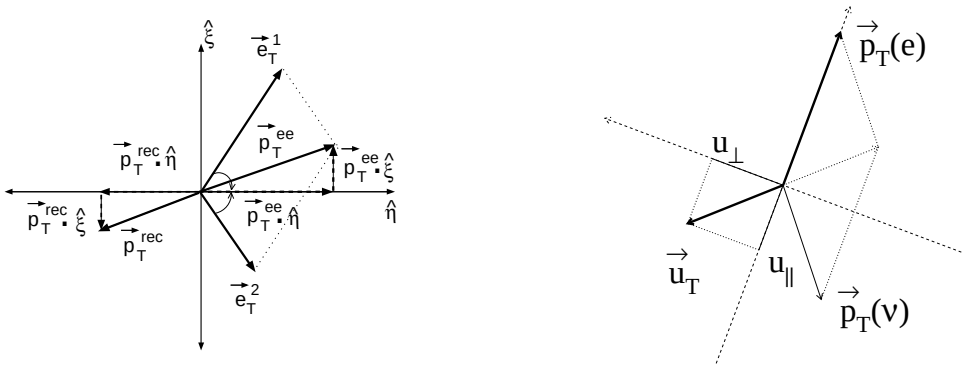

FIG. 1: Left: definitions of the $\hat{\eta}$ and $\hat{\xi}$ axes for $Z \to ee$ events. Right: definition of $u_\parallel$ and $u_\perp$ for $W \to e\nu$ events. $u_\parallel$ can be positive or negative, and is defined to be negative when opposite to the electron direction.

These tuning procedures were verified by performing a closure test using Monte Carlo W and Z events generated with the detailed GEANT simulation. These events were used to determine the PMCS parameters using the same methods as for data, and the W mass was then determined. The measured W mass agreed with the input value within the statistical uncertainty. Numerical results from this test are presented in Section VII.

A. Electron Efficiency Simulation

The electron selection efficiency can be discussed in terms of three contributions: (1) an intrinsic contribution arising from only the electron interaction in the detector, (2) a contribution from other activity in the event uncorrelated with the W production and decay and (3) effects from the W production itself. All three are modeled in PMCS by parametrizations derived using a combination of detailed simulation and data control samples.

The purely electron-related trigger, reconstruction, identification and track efficiencies are derived from the Z data control sample using the tag-and-probe method. As an example of this method, the tracking efficiency is measured by selecting $Z \to ee$ events in which two electrons are identified in the calorimeter. One of the electrons is required to have a matching track and pass the trigger selection. The fraction of such events in which the other electron has a matched track then defines the combined tracking reconstruction and matching efficiency. This method is applied in a sequential manner to measure the electron trigger, calorimeter-based identification and tracking efficiencies. In most cases, the absolute efficiency has limited impact on the result, and only effects which distort the shapes of the m_T, p_T^e and $\not\!\!E_T$ distributions impact this analysis. These efficiencies are parametrized as functions of η_e, p_T^e, and z_V where η_e is the electron pseudorapidity.

In addition to the electron-only effects, two other factors are important in determining the event-by-event efficiency. The first of these is the effect of additional hadronic energy in the calorimeter, typically arising from other $p\overline{p}$ interactions. This effect increases with increasing instantaneous luminosity because higher luminosity tends to increase the overall hadronic energy in the detector and thus reduce the electron finding efficiency. The reduction occurs because selection requirements depend on the shape of the energy deposition in the calorimeter and the relative amounts in the EM and hadronic sections. The second factor occurs because of correlations in the W event topology. The electron efficiency depends on the relative orientation of the hadronic recoil and the electron. The highest p_T^e values occur when the electron is back to back with the recoil, and the lowest values occur when the electron overlaps the recoil. When the recoil and electron overlap, the electron selection efficiency decreases. Thus, the final distributions are sculpted by this correlation.

Both of these effects are included in PMCS. The overall energy effect is parametrized using the event scalar transverse energy and $u_\parallel$. The scalar transverse energy is the scalar sum of the transverse energies of all calorimeter cells outside the electron window above a minimum energy and is denoted SET. The control sample for parametrizing this effect is events simulated by the GEANT simulation with zero bias (ZB) events added to account for the instantaneous luminosity effects. Zero bias events are chosen by a trigger requiring only synchronization with the beam crossing clock. The luminosity spectrum of the overlay events is chosen to match that of the data itself. Effects from spatial proximity of the recoil to the electron are parametrized using the electron p_T and $u_\parallel$ and these are determined using

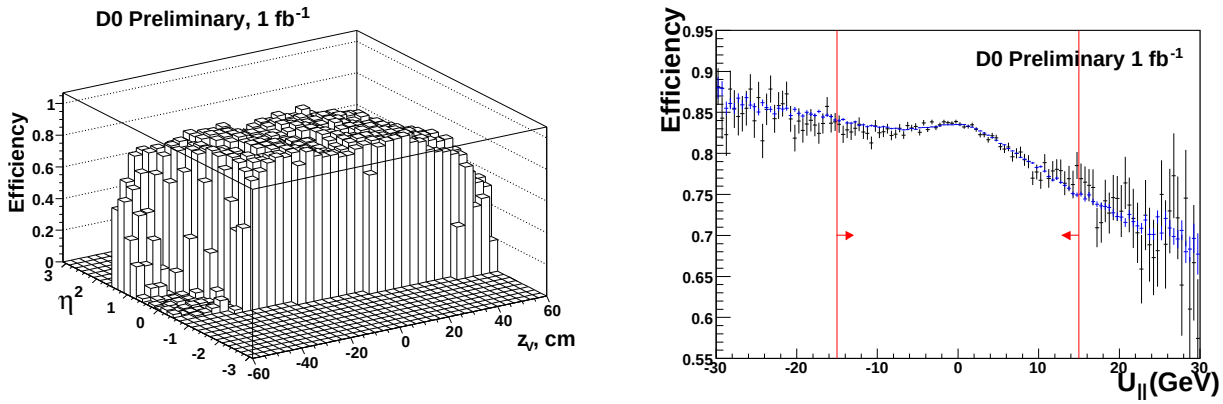

FIG. 2: The electron track efficiency as a function of η_e and z_V (left) and the electron efficiency as a function of $u_\parallel$ (right). The blue points are PMCS results, and the black points are Z data. The regions outside the two red lines are not used in this analysis.

the $Z \rightarrow ee$ control sample. Figure 2 shows the tracking efficiency as a function of η_e and z_V, and the electron efficiency as a function of $u_\parallel$ for data and PMCS Z events integrating over the p_T^e spectrum. The level of agreement of these these and related distributions results in only a 5 MeV systematic uncertainty on m_W.

B. Electron Response Simulation

The relationship between measured and true electron energy is given by

$$E = R_{EM}(E_0) \otimes \sigma_{EM}(E_0) + \Delta E(\mathcal{L}, u_\parallel) \tag{2}$$

where E_0 is the true electron energy, E is the reconstructed energy, $R_{EM}(E_0)$ is the response for a given E_0, σ_{EM} is the energy resolution for electromagnetic objects and $\Delta E(\mathcal{L}, u_\parallel)$ is a correction for energy included in the reconstructed electron energy which is not related to the electron energy deposition. This final correction is luminosity and topology dependent and is measured in W data from the energy observed in a region separated in phi from the electron.

The energy response of the EM calorimeter is modeled using

$$R_{EM}(E_0) = \alpha \times E_0 + \beta \tag{3}$$

where α is the response of the calorimeter to electrons and β is an offset which includes non-linear effects at low E_0 due to material in the detector. We determine α and β by fitting the Z mass distribution to that generated by PMCS for different α and β values. In obtaining these it is important that electrons from boosted Z's span a range of energies. Figure 3 shows the central values and one sigma contour for α and β determined from the fit. The fitted values are

$$\begin{aligned} \alpha &= 1.0111 \pm 0.0043 \\ \beta &= -0.40 \pm 0.21 \text{ GeV} \end{aligned}$$

and the correlation is -0.997. The large anticorrelation explains why the uncertainty on the W mass measurement from the electron energy calibration is much smaller than that of the β uncertainty alone.

The uncertainty on m_W arising from the α and β precision is determined by varying the parameters by the one sigma contour including the correlation and propagating the effect to the final W mass. The fit quality is good, so the α and β uncertainties are taken from the statistical uncertainties derived from the fit to $Z \rightarrow ee$ data. This is the dominant systematic uncertainty in the m_W measurement. Because it arises from the Z sample statistics this uncertainty should decrease as more data are collected.

The resolution of the EM calorimeter is modeled using the form

$$\frac{\sigma_{EM}(E)}{E} = \sqrt{C_{EM}^2 + \frac{S_{EM}^2}{E}} \tag{4}$$

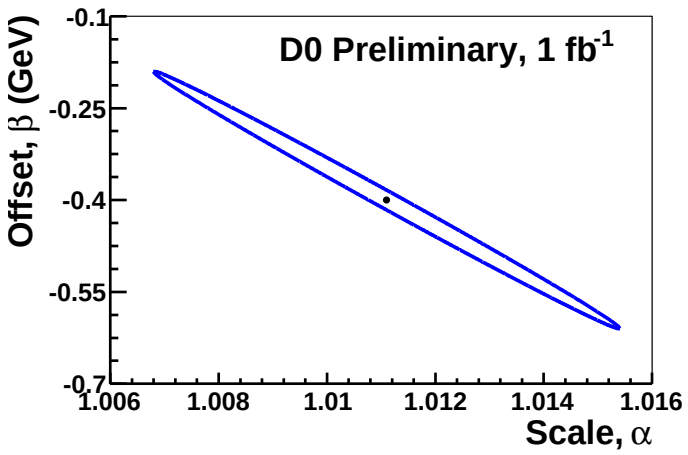

FIG. 3: The central value for α and β as determined from the fit to the Z mass distribution and the error ellipse defined by $\Delta\chi^2 = 1$.

where C_{EM} is the constant term and S_{EM} is the sampling term for the EM calorimeter[23]. Because of the large amount of material in front of the calorimeter, S_{EM} is not constant, but is parametrized as

$$S_{EM} = (S_1 + \frac{S_2}{\sqrt{E}}) \times \frac{e^{S_{exp}/\sin\theta}}{e^{S_{exp}}}$$

where

$$S_{exp} = S_3 - S_4/E - S_5^2/E^2$$

This formula and the constants $S_i,\ i = 1, ..., 5$ were derived using a GEANT simulation with significantly lower energy cut offs for particle propagation and updated interaction cross sections relative to the standard DØ simulation. Extra material in front of the calorimeter was also added to this simulation . The amount of material, nX_0, was determined by a χ^2 minimization of the difference between observed longitudinal profiles of electron showers in the calorimeter and those predicted by this special simulation. The result is $nX_0 = 0.1633 \pm 0.0095\ X_0$. The resulting full Monte Carlo was then used to update the energy calibration applied to data by the event reconstruction program.

The constant term, C_{EM}, was found using a fit of a Breit-Wigner line shape convoluted with a Gaussian to the Z peak. The Gaussian width characterizes the Z mass resolution. The value was derived by comparing the width of the Gaussian fitted to the Z peak predicted by the fast MC simulation and the data. The fast MC simulation has the functional form (Eq. 4) implemented for the energy resolution. The result from the fit is

$$C_{EM} = (2.04 \pm 0.13)\%$$

The fractional total resolution for a 50 GeV electron in the CC is roughly 3.6%. The uncertainty is propagated to the full W mass using standard techniques.

In addition, the need for a correction to account for different energy loss for electrons from W decay and those from Z decay was investigated. A difference could arise because W and Z electrons of the same energy have different pseudorapidity values and thus correspond to differences in material traversed. No need was found for a correction with a precision of 4 MeV, which is applied as a systematic uncertainty.

C. Recoil Response Simulation

The neutrino transverse momentum in W decay is inferred from the missing transverse energy ($\not\!\!E_T$). For data events, the $\not\!\!E_T$ is measured from the vector sum of the zero-suppressed calorimeter transverse energy deposition in each calorimeter cell within $|\eta| < 3.2$. It is modeled in the PMCS simulation as

$$-\vec{\not\!\!E}_T = \vec{p}_T(e) + \vec{u}_T \tag{5}$$

in which $\vec{p}_T(e)$ is the electron transverse momentum. The recoil, $\vec{u}_T$, is the vector sum of all transverse energy in the event not associated with the reconstructed electron. The recoil is modeled in PMCS using four components

$$\vec{u}_T = \vec{u}_T^{\,\mathrm{HARD}} + \vec{u}_T^{\,\mathrm{SOFT}} + \vec{u}_T^{\,\mathrm{ELEC}} + \vec{u}_T^{\,\mathrm{FSR}} \tag{6}$$

These components are:

- $\vec{u}_T^{\,\mathrm{HARD}} = \vec{f}(\vec{q}_T;\vec{\zeta})$
  Here $\vec{u}_T^{\,\mathrm{HARD}}$ denotes the recoil component associated with the hard scattering of the $q\bar{q}$ pair that resulted in the $W(Z)$ boson. This hard component balances the transverse momentum of the vector boson. Here $\vec{q}_T$ is the generator level momentum of the boson. The $\vec{f}(\vec{q}_T)$ is an ansatz function used for smearing the $\vec{q}_T$. It is derived from $Z \to \nu\nu$ GEANT Monte Carlo events. The simulated magnitude and direction are taken from a 2D probability distribution of Δq_T and $\Delta\phi$ parametrized as a function of the true q_T. Here the Δ values are differences between the measured and true values in the $Z \to \nu\nu$ simulated events. The $\vec{\zeta}$ is a five element parameter vector used to perform the final fine-tuning of the recoil response and resolution using data control samples.

- $\vec{u}_T^{\,\mathrm{SOFT}} = -\rho_{MB} \cdot \vec{\not\!\!E}_T^{\,\mathrm{MB}} - \vec{\not\!\!E}_T^{\,\mathrm{ZB}}$
  Here $\vec{u}_T^{\,\mathrm{SOFT}}$ represents the other interactions that contribute to the hadronic recoil. The first part is from the underlying event, and the second is the additional energy content in the event. The underlying event energy is defined to be that from the interactions of the remaining (or spectator) partons of the same $p\bar{p}$ pair that produced the vector boson. It is modeled using data minimum bias (MB) events with only one reconstructed primary vertex. Minimum bias events are chosen by a trigger requiring hits in both luminosity counters which are in time with a beam crossing. The additional energy content is associated with all the other interactions occurring in the $p\bar{p}$ pairs present in the same or previous beam crossings. Interactions contributing to detector noise are also included in this sub-component. It is modeled using data ZB events. The parameter ρ_{MB} is a scale factor determined by fitting the observed SET distribution to predictions generated by PMCS with differing ρ_{MB} values.

- $\vec{u}_T^{\,\mathrm{ELEC}} = -\sum_e \Delta u_{\parallel} \cdot \hat{p}_T(e)$
  This component gives a correction for the recoil energy that is parallel to the electron direction. The recoil energy present within the electron window is measured as part of the electron energy and is thus subtracted from the recoil energy. This correction is determined in W data events using distributions of energy measured in an equal sized window azimuthally separated from the electron and hadronic recoil direction as described in Section V B.

- $\vec{u}_T^{\,\mathrm{FSR}} = \sum_\gamma \vec{p}_T(\gamma)$
  This component contains the energy of final state radiation (FSR) photons that are far away from the electron and hence reconstructed as recoil energy.

These four components are derived using detailed simulation and data events. Because the simulation alone is not expected to reproduce the true hard recoil with sufficient precision, the recoil model is then further tuned using data $Z \to ee$ events. The sum of the recoil $\vec{u}_T$ and dielectron momentum $\vec{p}_T^{\,ee}$ vectors in Z events is projected on to the $\hat{\eta}$ and $\hat{\xi}$ axes defined earlier. The recoil model is then tuned using the imbalance of recoil and electron energy in the $\hat{\eta}$ projection (Fig. 1), called η_{imb}. The η_{imb} mean is used to fine tune the recoil response, and the η_{imb} width is used to fine tune the recoil resolution. By construction, the vector $\hat{\eta}$ is insensitive to the electron energy measurement. The tuning involves five parameters, and the parameters for the response and resolution were determined independently of each other. Figure 4 shows the mean and width of η_{imb} for data and the tuned PMCS as functions of p_T^{ee}. The χ^2/dof for the response fit is 3.1/7 and for the resolution fit is 4.5/8.

The systematic uncertainties arising from the recoil model are determined by propagating the uncertainties on the five tuning parameters derived from the fits. The fits have good χ^2 values, so, as for the electron response and resolution, these uncertainties are dominated by the statistics of the Z control sample.

VI. BACKGROUNDS

There are three significant backgrounds in the W sample: (1) $Z \to ee$ events in which one electron escaped in a poorly instrumented region of the detector, (2) multijet events (QCD) in which a jet is misidentified as an electron and $\not\!\!E_T$ arises from misreconstruction and (3) $W \to \tau\nu \to e\nu\nu$ events. The first two components are measured using control data samples, and the third is estimated using simulation.

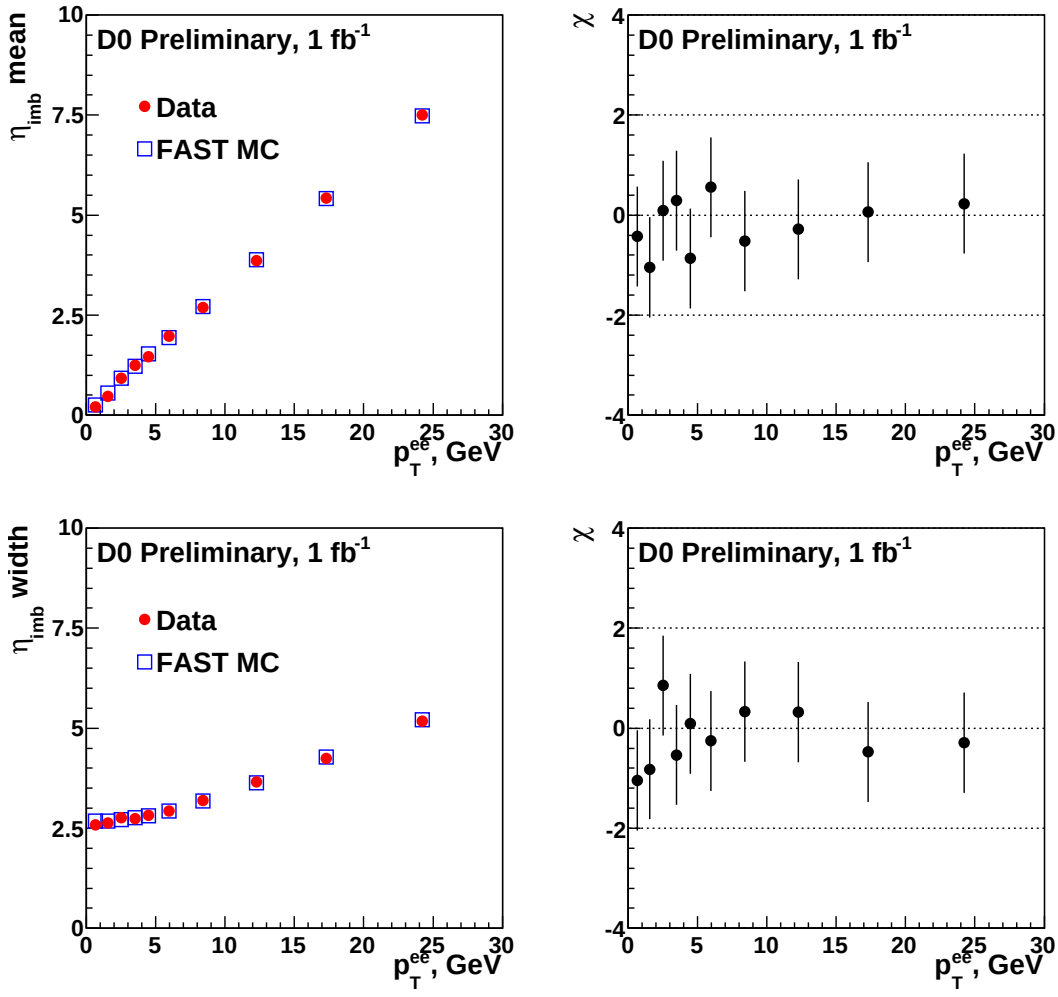

FIG. 4: The mean (upper left) and width (lower left) of η_{imb} as functions of p_T^{ee} and the χ values (right, upper and lower) for the difference between data and PMCS are shown.

The Z background arises mainly from electrons which traverse the gap between the central and end calorimeters. The tracking efficiency in this region is good, so this background is estimated by selecting events passing the standard W selection additionally requiring a track back-to-back in azimuth with the detected electron that has a charge with a sign opposite to the charge of the detected electron. The track must also be in the gap region $1.0 < |\eta_{det}| < 1.5$. The Z background estimate obtained is $(0.80 \pm 0.01)\%$. The shapes of the kinematic distributions arising from this background are also taken from the control sample.

The QCD background is determined using a sample obtained by removing the matching track requirement. This sample contains the W events, but has a significantly higher contamination from QCD background than the standard sample. The probabilities for W events and for multijet events to have a matched track are determined in control samples. The W probability is determined from Z data, and the QCD probability is determined from EM+jet events in which the EM candidate passes the full trigger and electron identification requirements used in this analysis except no track match is initially required. The number of events in the sample without the track requirement and the two probabilities are then used to determine the number of QCD background events in the final W sample. The QCD background level is found to be $(1.49 \pm 0.03)\%$. The shapes of the kinematic distributions used in the mass fit are taken from the loose selection after subtracting the W contribution.

The $W \to \tau\nu \to e\nu\nu$ contribution is determined from detailed simulation of the process using the DØ full simulation chain. Because the electron arises from a secondary decay, the momenta are lower than that from direct $W \to e\nu$ and the distribution is broader. The background contribution from $W \to \tau\nu$ is $(1.60 \pm 0.02)\%$. The three background contributions with proper normalization are shown in Fig. 5.

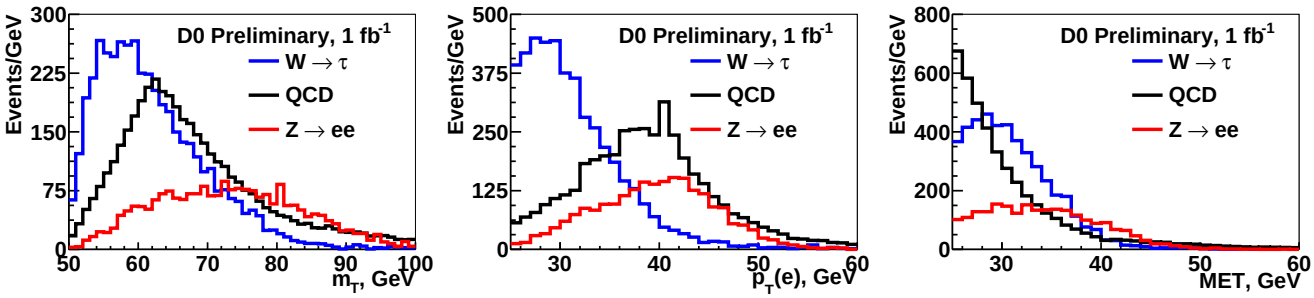

FIG. 5: The m_T, p_T^e and $\not\!\!E_T$ distributions for the three backgrounds Z(red), QCD(black) and $W \to \tau\nu$(blue) with absolute normalization. (color online)

VII. MASS FITS AND RESULTS

The W mass is determined by fitting each of the data m_T, p_T^e and $\not\!\!E_T$ distributions to corresponding distributions generated using PMCS. The PMCS distributions (templates) are generated at a series of input W mass values with 10 MeV steps and backgrounds added to the simulated distributions. A binned likelihood between the data and template is then computed for each template. The resulting log likelihoods from each mass point(template) are then fit to a parabola to determine the best fit W mass. The fits are performed separately for each of the m_T, p_T^e and $\not\!\!E_T$ distributions.

A test of the analysis procedure was performed using events produced by the standard DØ full Monte Carlo simulation treated as collider data. The methods used for the data analysis were applied to the simulated events in this Monte Carlo test, including performing the Z boson-based tuning using simulated events. PMCS was separately tuned for this study to describe the full Monte Carlo. The differences Δm_W between the fitted results and input W mass value of 80.450 GeV are $\Delta m_W = 0.009 \pm 0.015(\text{stat}) \pm 0.011 \pm 0.010$ GeV, $\Delta m_W = 0.009 \pm 0.017(\text{stat}) \pm 0.007 \pm 0.010$ GeV and $\Delta m_W = 0.016 \pm 0.017(\text{stat}) \pm 0.010 \pm 0.010$ GeV for the m_T, p_T^e and $\not\!\!E_T$ fits respectively. The first uncertainty arises from W statistics in the full Monte Carlo sample, the second uncertainty arises from the statistics of the Z used in the tuning, and the third uncertainty arises from residual differences in energy loss corrections arising because electrons in the full Monte Carlo sample from W decay have different energy and η distributions than those from Z decay.

During the PMCS tuning for the collider data analysis, the W mass returned from fits was blinded by the addition of an unknown constant offset until the analysis was finalized. This allowed the full tuning on the Z and W events and internal consistency checks to be performed without developing any knowledge of the final result. Once all distributions were of sufficient quality the results were unblinded. The Z mass fit is shown in Fig. 6. For an input value $m_Z = 91.188$ GeV used in the tuning, the value returned from the post-tuning fit was 91.185 ± 0.033(stat). After unblinding, the W mass fit results from data are given in Table I. The distributions of each variable showing the

Variable	Fit Range (GeV)	Result (GeV)	χ^2/dof
m_T	$65 < m_T < 90$	80.401 ± 0.023	48/49
p_T^e	$32 < p_T^e < 48$	80.400 ± 0.027	39/31
$\not\!\!E_T$	$32 < \not\!\!E_T < 48$	80.402 ± 0.023	32/31

TABLE I: Results from the fits to data. The uncertainty is only the statistical component. The χ^2/dof values are computed over the fit range.

data and PMCS template with background for the best fit value are shown in Fig. 7 through Fig. 9. These figures also show the bin-by-bin χ values defined as the difference between the data and template divided by the data uncertainty and show the likelihood as a function of assumed W mass.

A. Systematic Uncertainties

The systematic uncertainties in the W mass measurement arise from a variety of sources, but can roughly be categorized as those arising from experimental sources and those arising from theory. The methods used to derive the systematic uncertanties have been described in the corresponding sections above. The systematic uncertainties are

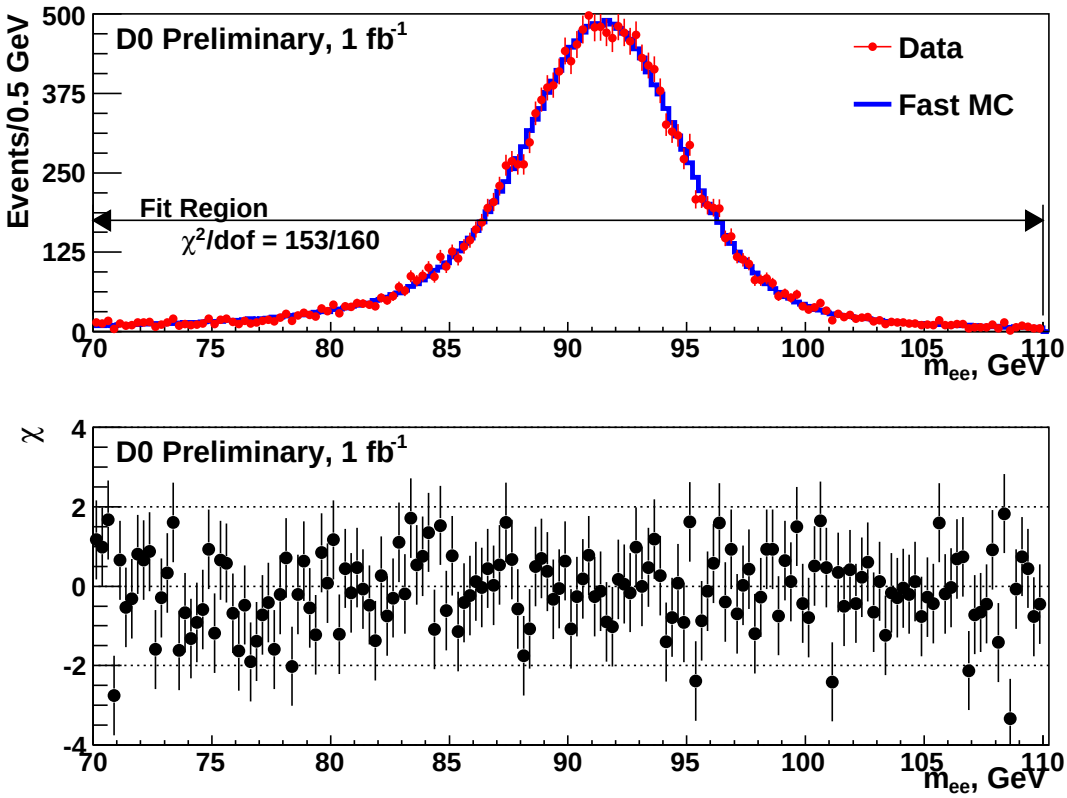

FIG. 6: The Z mass distribution in data and from the fast simulation PMCS (top) and the χ values for each bin (bottom). The agreement is quite good, giving $\chi^2/\text{dof} = 153/160$.

summarized in Table II. The largest uncertainty, 34 MeV arises from the precision with which the electron energy scale is known. This is limited by the statistical power of the $Z \to ee$ sample, and it is expected to improve with more data.

B. Consistency checks

An indication of the quality with which our data are properly understood can be seen in the excellent agreement between the data and PMCS m_{ee} distribution shown in Fig. 6, the χ plots in Figs. 7 through 9 and in the recoil variables shown in Fig. 4.

To further check the stability of the result, the fits were repeated by changing the range shown in column 2 of Table I over which the fits were performed relative to the default values. Figure 10 shows the variation resulting from these tests applied to the m_T distribution. The result is stable to within our uncertainty as a function of varying the fit range. The data were also subdivided into statistically independent categories based on instantaneous luminosity, time, SET, $u_\parallel$, $u_\perp$ and η_e range. The result is stable within one standard deviation for each of these variations.

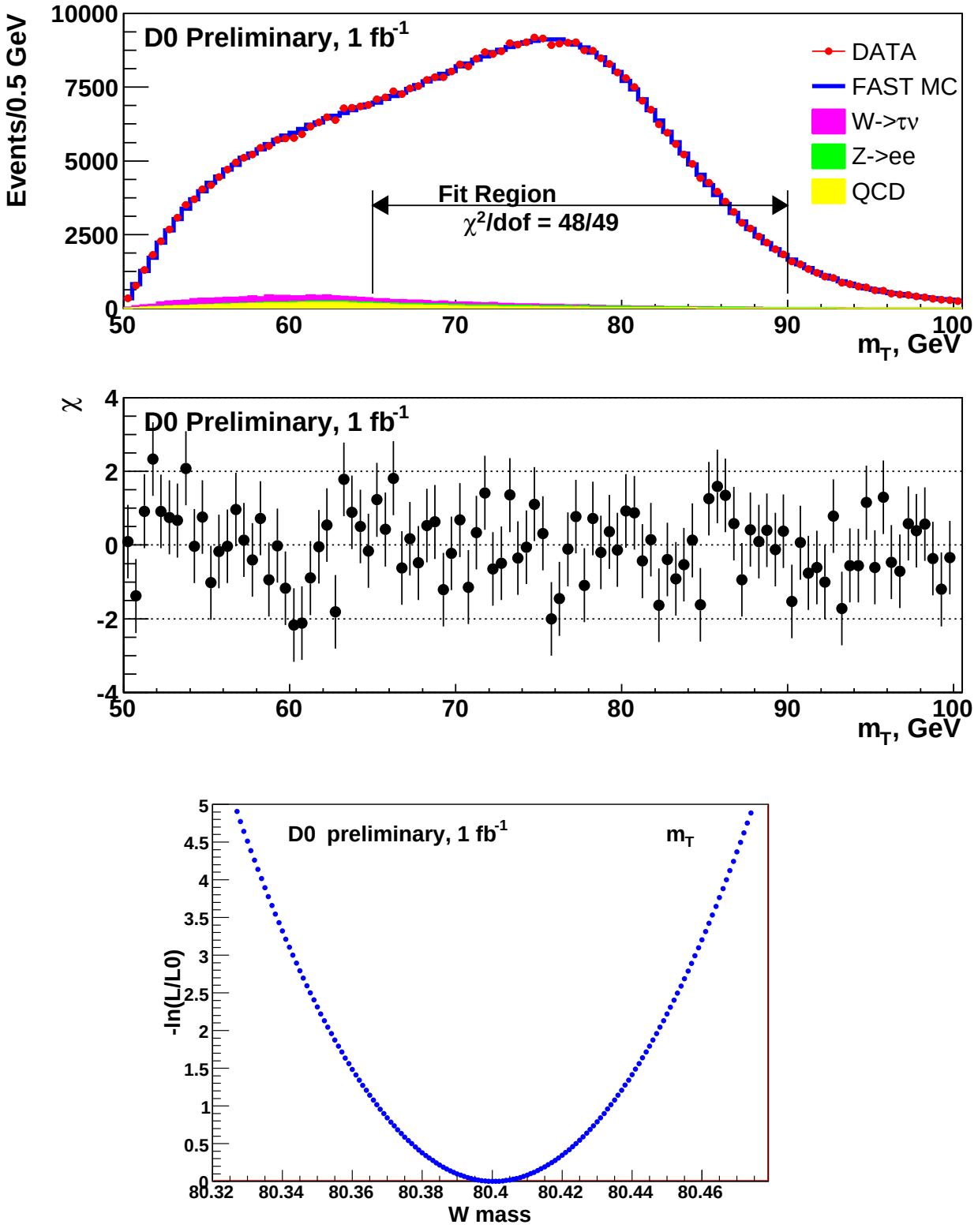

FIG. 7: The m_T distribution for data and PMCS simulation with backgrounds added (top), the χ value for each bin (center) and the negative log of the likelihood ratio L/L_0 where L_0 is the maximum likelihood as a function of m_W (bottom).

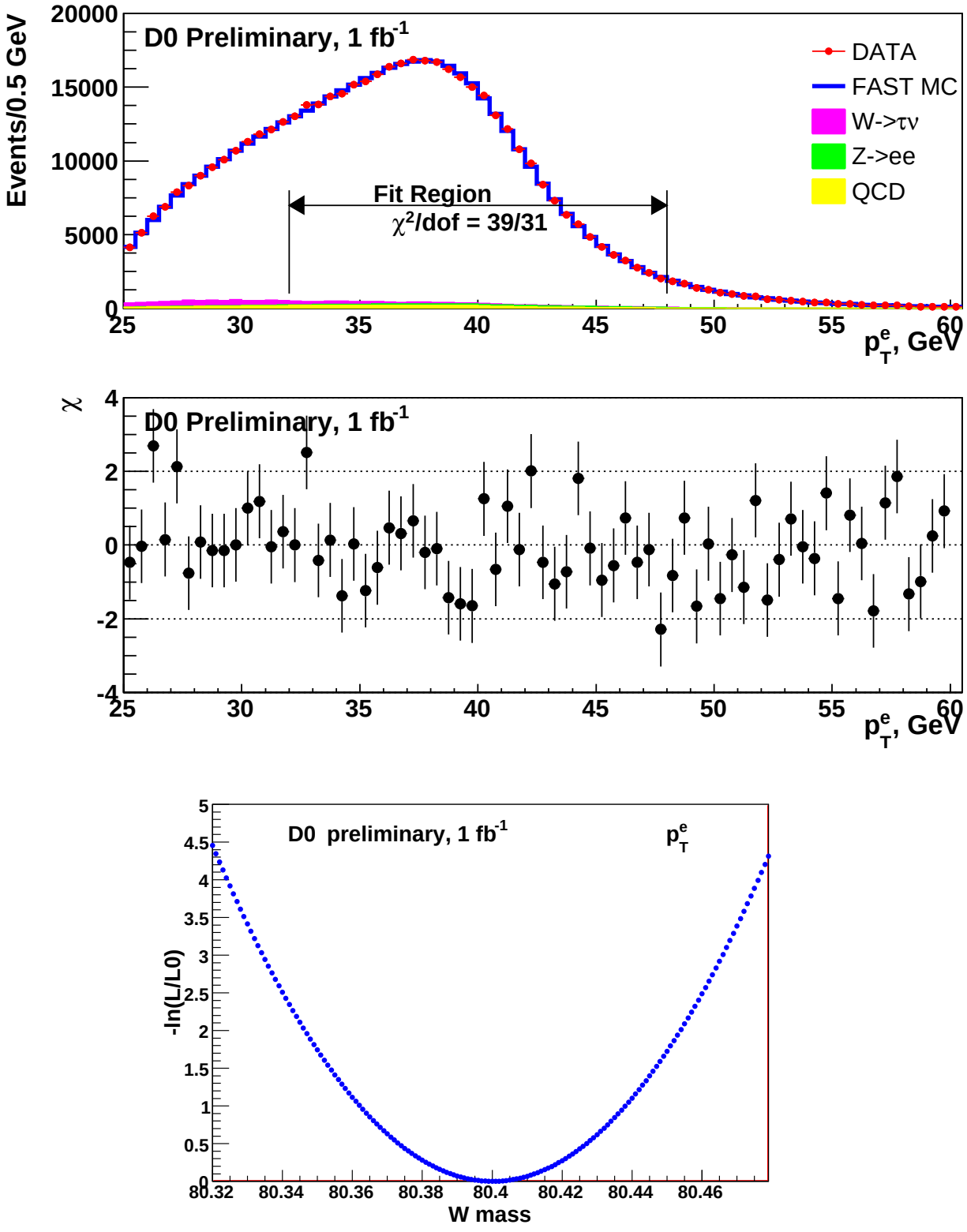

FIG. 8: The p_T^e distribution for data and PMCS simulation with backgrounds added (top), the χ value for each bin (center) and the negative log of the likelihood ratio L/L_0 where L_0 is the maximum likelihood as a function of m_W(bottom).

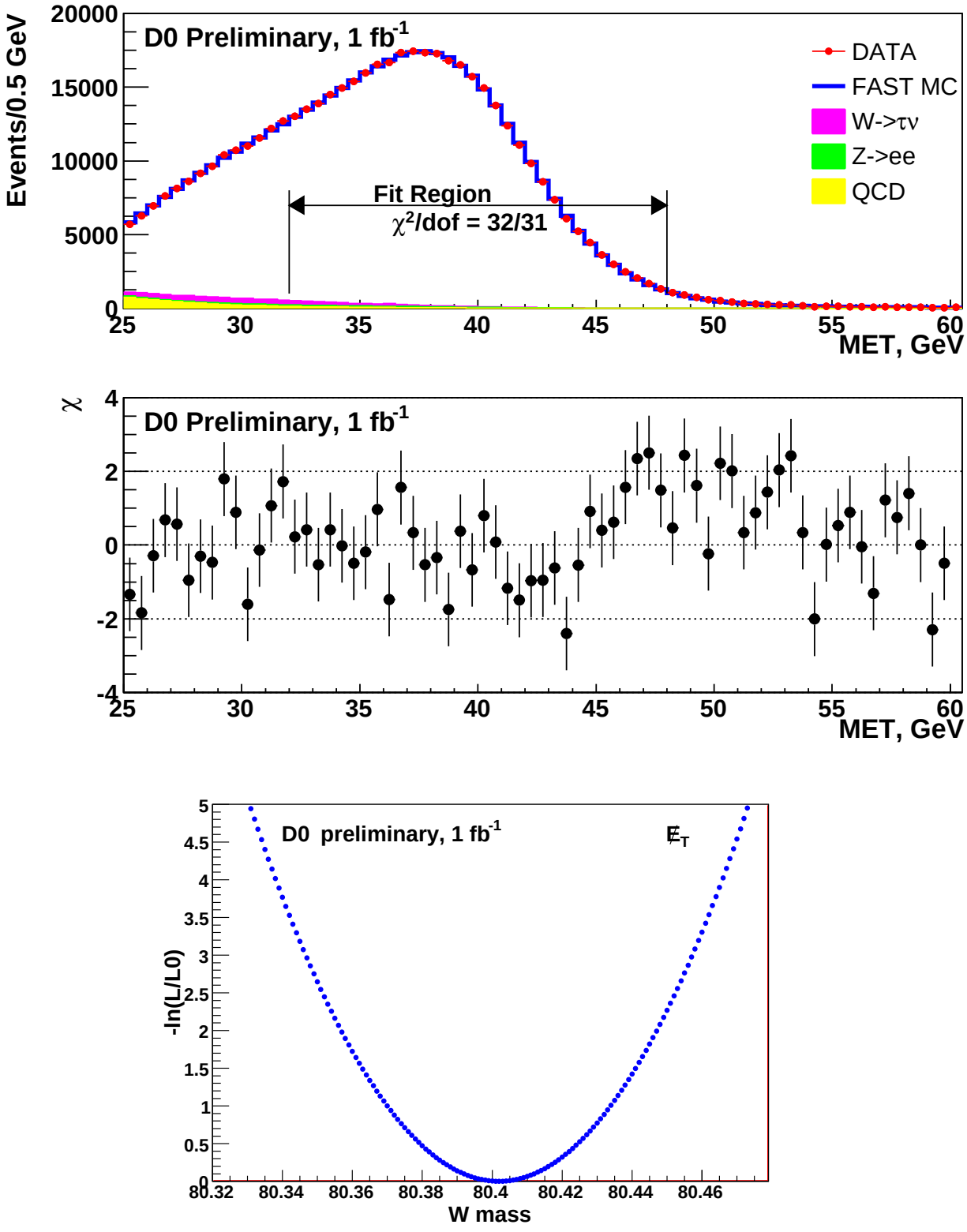

FIG. 9: The $\not\!\!E_T$ distribution for data and PMCS simulation with backgrounds added (top), the χ value for each bin (center) and the negative log of the likelihood ratio L/L_0 where L_0 is the maximum likelihood as a function of m_W (bottom).

Source	$\sigma(m_W)$ MeV m_T	$\sigma(m_W)$ MeV p_T^e	$\sigma(m_W)$ MeV $\not\!\!E_T$
Experimental			
Electron Energy Scale	34	34	34
Electron Energy Resolution Model	2	2	3
Electron Energy Nonlinearity	4	6	7
W and Z Electron energy loss differences	4	4	4
Recoil Model	6	12	20
Electron Efficiencies	5	6	5
Backgrounds	2	5	4
Experimental Total	35	37	41
W production and decay model			
PDF	9	11	14
QED	7	7	9
Boson p_T	2	5	2
W model Total	12	14	17
Total	37	40	44

TABLE II: Systematic uncertainties on the W mass results. The dominant systematic uncertainty comes from the electron energy scale, and this is determined by the statistical power of the Z event sample.

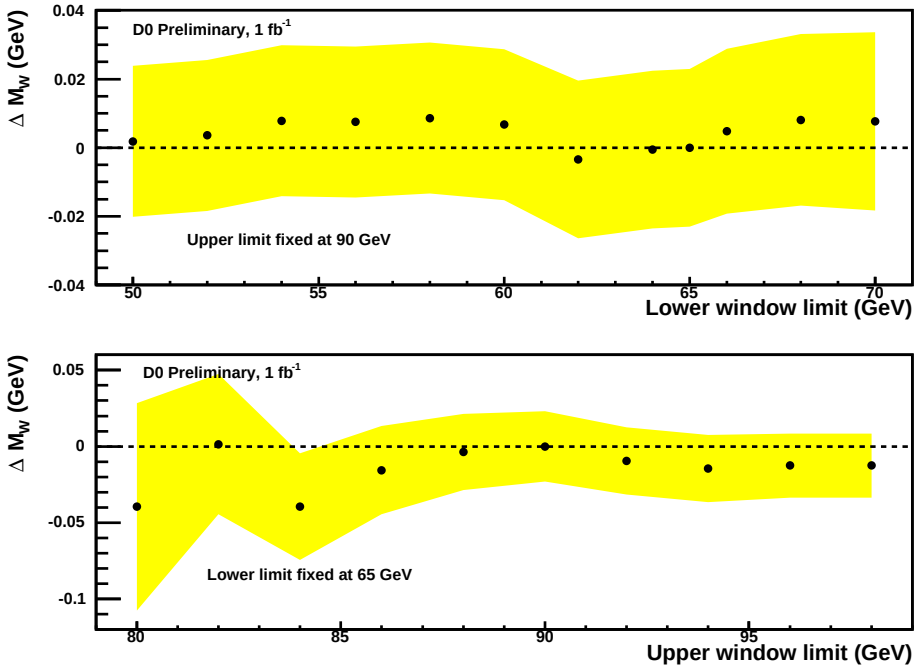

FIG. 10: Variation in the mass determined from fits to the m_T spectrum as the fit range was changed. The yellow band indicates the statistical uncertainty.

C. Combination

The measurements from the three methods are correlated. Ensemble tests and standard uncertainty propagation methods are used to determine the correlation matrix which is found to be

$$\rho = \begin{pmatrix} \rho_{m_T m_T} & \rho_{m_T p_T^e} & \rho_{m_T \not\!\!E_T} \\ \rho_{m_T p_T^e} & \rho_{p_T^e p_T^e} & \rho_{p_T^e \not\!\!E_T} \\ \rho_{m_T \not\!\!E_T} & \rho_{p_T^e \not\!\!E_T} & \rho_{\not\!\!E_T \not\!\!E_T} \end{pmatrix} = \begin{pmatrix} 1.0 & 0.83 & 0.82 \\ 0.83 & 1.0 & 0.68 \\ 0.82 & 0.68 & 1.0 \end{pmatrix}$$

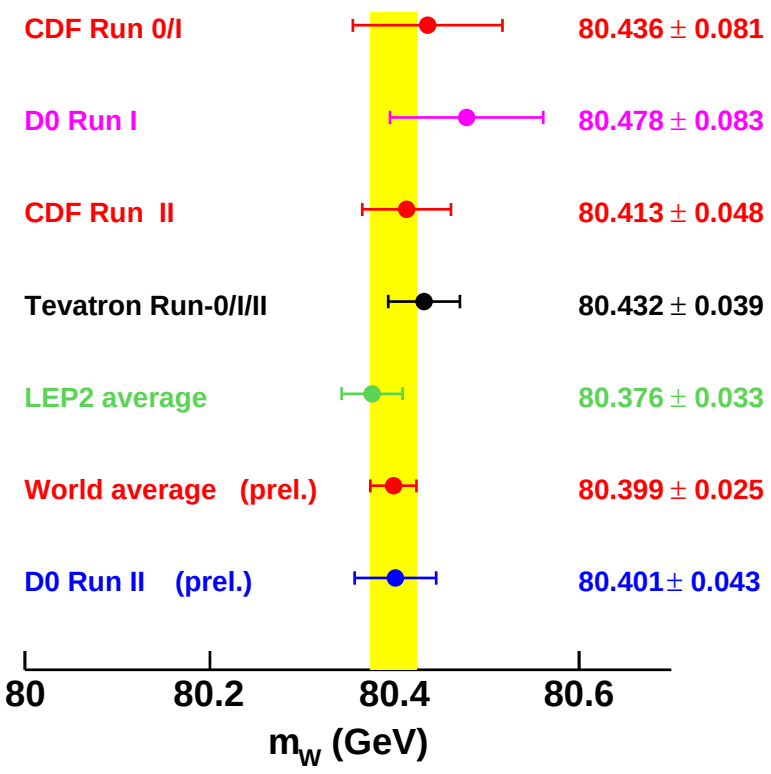

FIG. 11: A comparison of the result presented here, the world average (without this result) and the measurements used in determining the world average. [1, 20]

The measurements are combined [21] using this correlation, and the result is

$$m_W = 80.401 \pm 0.021 \text{ (stat)} \pm 0.038 \text{ (syst) GeV} = 80.401 \pm 0.043 \text{ GeV}.$$

VIII. CONCLUSIONS

The W boson mass has been measured using the $W \to e\nu$ mode and 1 fb^{-1} of DØ data taken between 2002 and 2006. The mass was measured using three different kinematic variables m_T, p_T^e and $\not\!\!E_T$. The three measurements were combined to give the result

$$m_W = 80.401 \pm 0.021 \text{ (stat)} \pm 0.038 \text{ (syst) GeV} = 80.401 \pm 0.043 \text{ GeV}.$$

Figure 11 shows this result, the world average and the results used to compute the world average. The new DØ result is in good agreement with these measurements.

Acknowledgments

We thank the staffs at Fermilab and collaborating institutions, and acknowledge support from the DOE and NSF (USA); CEA and CNRS/IN2P3 (France); FASI, Rosatom and RFBR (Russia); CNPq, FAPERJ, FAPESP and FUNDUNESP (Brazil); DAE and DST (India); Colciencias (Colombia); CONACyT (Mexico); KRF and KOSEF (Korea); CONICET and UBACyT (Argentina); FOM (The Netherlands); STFC (United Kingdom); MSMT and GACR (Czech Republic); CRC Program, CFI, NSERC and WestGrid Project (Canada); BMBF and DFG (Germany); SFI (Ireland); The Swedish Research Council (Sweden); CAS and CNSF (China); and the Alexander von Humboldt Foundation (Germany).

[1] The LEP ElectroWeak Working Group, CERN-PH-EP/2008-20; arXiv:0811.4682 [hep-ex] (2008).
[2] S. Schael *et al.* (ALEPH Collaboration), Eur. Phys. J. C **47**, 309 (2006).
[3] J. Abdallah *et al.* (DELPHI Collaboration), Eur. Phys. J. C **55**, 1 (2008); arXiv:0803.2534v1 [Eur. Phys. J. C (to be published)].
[4] P. Achard *et al.* (L3 Collaboration), Eur. Phys. J. C **45**, 569 (2006).
[5] G. Abbiendi *et al.* (OPAL Collaboration), Eur. Phys. J. C **45**, 307 (2006).
[6] V. M. Abazov *et al.* (D0 Collaboration), Phys. Rev. D **66**, 012001 (2002); B. Abbott *et al.* (D0 Collaboration), Phys. Rev. D **58**, 092003 (1998); B. Abbott *et al.* (D0 Collaboration), Phys. Rev. D **62**, 092006 (2000).
[7] T. Affolder *et al.* (CDF Collaboration), Phys. Rev. D **64**, 052001 (2001).
[8] T. Aaltonen *et al.* (CDF Collaboration), Phys. Rev. Lett. **99**, 151801 (2007); T. Aaltonen *et al.* (CDF Collaboration), Phys. Rev. D **77**, 112001 (2008).
[9] V.M. Abazov *et al.* (DØ Collaboration), Nucl. Instrum. Methods Phys. Res. A **565**, 463 (2006).
[10] C. Amsler et al., Physics Letters B **667**, 1 (2008) and references therein.
[11] C. Balazs and C.P. Yuan, Phys. Rev. D **56**, 5558 (1997).
[12] F. Landry, R.Brock, P. Nadosky, C.P. Yuan, Phys. Rev. D **67**, 073016 (2003); V. Abazov *et al.*, Phys. Rev. Lett. **100**, 102002 (2008).
[13] E. Barbiero and Z. Was, Comp. Phys. Commun. **79**, 291 (1994).
[14] U. Baur, S. Keller and D. Wackeroth, Phys. Rev. D **59** 013002 (1999).
[15] U. Baur, S. Keller and D. Wackeroth, "A Monte Carlo program for the calculation of electroweak radiative corrections to Z boson production at hadron colliders", Available at `http://ubhex.physics.buffalo.edu/~baur/zgrad2.tar.gz`
[16] H.L. Lai *et al.*, Phys. Rev. D **55**, 1280 (1997); J. Pumplin *et al.*, JHEP **0310**, 046 (2003);
[17] T. Sjöstrand *et al.*, Comput. Phys. Commun. **135**, 238 (2001).
[18] R. Brun and F. Carminati, CERN Program Library Long Writeup W5013 (1993).
[19] UA2 Collaboration, J. Alitti et al., Phys. Lett. B **276**, 354 (1992).
[20] The Tevatron Electroweak Working Group, "Combination of CDF and DØ Results on the W Boson Mass and Width" FERMILAB-TM-2415 1^{st} August 2008. More information is available at: http://tevewwg.fnal.gov.
[21] L. Lyons, D. Gibout, and P. Clifford, Nucl. Instrum. Methods in Phys. Res. A **270**, 110 (1988).
[22] Throughout this note, we adopt the convention $\hbar = c = 1$.
[23] The standard form also has a noise term N that depends on N/E. This term has a negligible impact and is ignored.